

The universal rotation curve of spiral galaxies – II. The dark matter distribution out to the virial radius

P. Salucci,^{1*} A. Lapi,¹ C. Tonini,¹ G. Gentile,² I. Yegorova¹ and U. Klein³

¹SISSA International School for Advanced Studies, via Beirut 4, I-34013 Trieste, Italy

²University of New Mexico, Department of Physics and Astronomy, 800 Yale Blvd NE, Albuquerque, NM 87131, USA

³Argelander-Institut für Astronomie, Auf dem Hügel 71, D-53121 Bonn, Germany

Accepted 2007 March 5. Received 2007 February 16; in original form 2006 November 24

ABSTRACT

In the current Λ CDM cosmological scenario, N -body simulations provide us with a universal mass profile, and consequently a universal equilibrium circular velocity of the virialized objects, as galaxies. In this paper we obtain, by combining kinematical data of their inner regions with global observational properties, the universal rotation curve of disc galaxies and the corresponding mass distribution out to their virial radius. This curve extends the results of Paper I, concerning the inner luminous regions of Sb–Im spirals, out to the edge of the galaxy haloes.

Key words: galaxies: formation – galaxies: haloes – galaxies: kinematics and dynamics – dark matter.

1 INTRODUCTION

Rotation curves (hereafter RCs) of disc galaxies do not show any Keplerian fall-off and do not match the distribution of the stellar (plus gaseous) matter. As a most natural explanation, this implies an additional invisible mass component (Rubin et al. 1980; Bosma 1981; Persic & Salucci 1988) that becomes progressively more conspicuous for the less luminous galaxies (e.g. Persic & Salucci 1988, 1990; Broeils 1992a). Moreover, the kinematical properties of Sb–Im spirals lead to the concept of the *universal rotation curve* (URC) implicit in Rubin et al. (1985), pioneered in Persic & Salucci (1991) and set in Persic et al. (1996, hereafter PSS, Paper I): RCs can be generally represented out to R_f , the outermost radius where data are available, by $V_{\text{URC}}(R; P)$, that is, by a *universal* function of radius, tuned by some galaxy property P . P can be a global property such as the luminosity and the disc or halo mass or a well-defined local quantity like V_{opt} . In any case it serves as the galaxy identifier. In PSS individual RCs and a number of co-added RCs proved the URC paradigm being well fitted by an analytical Curve, $V_{\text{URC}}(r/R_{\text{opt}}, L)$,¹ a function which is the sum in quadrature of two terms: V_{URCD} and V_{URCH} , each representing the disc or halo contribution to the circular velocity:

$$V_{\text{URC}}^2 = V_{\text{URCD}}^2 + V_{\text{URCH}}^2. \quad (1)$$

The stellar component was described by a Freeman disc (Freeman 1970) of surface density $\Sigma_{\text{D}}(r) = \frac{M_{\text{D}}}{2\pi R_{\text{D}}^2} e^{-r/R_{\text{D}}}$ and contributing to the circular velocity V as

$$V_{\text{URCD}}^2(x) = \frac{1}{2} \frac{GM_{\text{D}}}{R_{\text{D}}} (3.2x)^2 (I_0 K_0 - I_1 K_1), \quad (2a)$$

where $x = r/R_{\text{opt}}^2$ and I_n and K_n are the modified Bessel functions computed at $1.6x$. The dark matter component (with $V_{\text{URCH}}^2(r) = \frac{GM_{\text{H}}(<r)}{r}$) was described by means of a simple halo velocity profile:

$$V_{\text{URCH}}^2(x) = \frac{1}{4\pi} \frac{G\rho_0 a^2 x^2}{a^2 + x^2}. \quad (2b)$$

The above implies a density profile with an inner flat velocity core of size $\sim aR_{\text{opt}}$, a central density ρ_0 , an outer r^{-2} decline. The sum of the contributions (2a) and (2b) well fit all the PSS data with ρ_0, a^2 specific functions of luminosity (see PSS). Let us remind that disc masses M_{D} of spirals were found in the range $10^9 M_{\odot} \leq M_{\text{D}} \leq 2 \times 10^{11} M_{\odot}$.

The URC for the purpose of this work matches well the individual RCs of late-type spirals (see also Appendix for a discussion). It is useful to express the URC paradigm in the following way: at any chosen radius, the URC predicts the circular velocity of a (late-type) spiral of *known* luminosity and disc scalelength, within an error that is one order of magnitude smaller than the variations it shows (i) at different radii and (ii) at any radius, with respect to objects of different luminosity.

Let us remind the reader that the universal curve built in PSS holds out to R_f , and uses the luminosity as the galaxy identifier and the disc scalelength as a unit of measure for the radial coordinate. We will label it as URC_0 to indicate it as the first step of a definitive function of the dark radial coordinate, able to reproduce the observed RCs of spirals. URC_0 provides fundamental information on the mass distribution (MD) in spirals, while it suffers from three limitations: (1) it strictly holds only in a region extended less than 5 per cent the DM halo size (see below) (2) the velocity profile of the halo component, valid out to R_f , cannot be extrapolated to radii of

*E-mail: salucci@sisssa.it

¹ The reader is directed to PSS for the details of the procedure.

² We define the ‘disc size’ $R_{\text{opt}} \equiv 3.2 R_{\text{D}}$.

cosmological interest 3) it identifies objects by their luminosities, rather than by their virial masses. Let us point out that the URC₀ has been often and successfully used as an observational benchmark for theories, but this, only for $R < R_l$ and after that a relation between the halo mass and the galaxy luminosity was assumed.

On the other side, high-resolution cosmological N -body simulations have shown that, within the Lambda cold dark matter (Λ CDM) scenario, dark haloes achieve a specific equilibrium density profile characterized by a universal shape and, in turn, a universal halo circular velocity (Navarro, Frenk & White 1996, NFW), $V_{\text{NFW}}(R, M_{\text{vir}})$ in which the virial mass M_{vir} and virial radius R_{vir} are the galaxy identifier and radial coordinate.

$$\rho_{\text{H}}(r) = \frac{M_{\text{vir}}}{4\pi R_{\text{vir}}^3} \frac{c^2 g(c)}{x(1+cx)^2}, \quad (3a)$$

where $x \equiv r/R_{\text{vir}}$ is the radial coordinate, c is the concentration parameter, and $g(c) = [\ln(1+c) - c/(1+c)]^{-1}$. The parameter c is found to be a weak function of the halo mass, given by $c \approx 14 (M_{\text{vir}}/10^{11} M_{\odot})^{-0.13}$ (Bullock et al. 2001; Dutton 2006). This leads to

$$V_{\text{NFW}}^2(r) = V_{\text{vir}}^2 \frac{c}{g(c)} \frac{g(x)}{x}, \quad (3b)$$

with $V_{\text{vir}} = V(R_{\text{vir}})$. It is interesting to note that in this scenario the present-day circular velocity, which also includes a baryonic component arranged in a disc, is predicted to be a *universal* function of radius, tuned by few galaxy parameters (Mo, Mao & White 1998). However, it is well known that observations of spiral galaxies favour density concentrations lower than those predicted for CDM by equation (3a): DM haloes detected around spirals do not show the NFW central cusp in favour of a core-like structure (van den Bosch & Swaters 2001; Swaters et al. 2003; Weldrake et al. 2003; Donato et al. 2004; Gentile et al. 2005; Simon et al. 2005; Gentile et al. 2007).

Therefore, the reconstruction of the MD of DM haloes from observations *in parallel* with that emerging from N -body simulations is required not only as a normal scientific routine, but also in view of a likely theory-versus-observations disagreement.

As an alternative to the simulation method, we will support the URC paradigm by means of a set of proper observational data and we will derive an analytical form for this curve, valid from the galaxy centre out to its virial radius and characterized by the halo mass as the galaxy identifier. In detail, we extend/improve the URC₀ in PSS (i) by adopting a different halo profile, proper to describe the halo distribution out to the virial radius, (ii) by using a number of RCs substantially more extended than those in PSS and (iii) by exploiting the relationship between the disc mass M_{D} , and the virial galaxy mass M_{vir} , recently obtained by Shankar et al. (2006). This will allow to build an ‘observational’ universal curve, $V_{\text{URC}}(R; M_{\text{vir}})$, extended out to R_{vir} and having the virial mass as the galaxy identifier. This curve is the observational counterpart of the universal Λ CDM NFW N -body generated profile.

Although the concept behind the URC may be valid also for galaxies of different Hubble types (see Salucci & Persic 1997), a number of issues are still open and will be dealt elsewhere:

(i) Sa galaxies amount, by number, to less than 10 per cent of the whole spiral population, and are important objects in view of the dual nature of their stellar distribution. They show RC profiles with a clear systematics with luminosity (Rubin et al. 1985), but, not unexpectedly, with some difference from those of the URC₀ (Noordermeer 2007).

(ii) Dwarf spirals with $V_{\text{opt}} < 50 \text{ km s}^{-1}$ are not well studied and included in the URC yet, also because in these objects the RCs do not coincide with the circular velocity, being significant the complex asymmetric drift correction.

(iii) The kinematical properties of spirals of very high stellar disc mass are not presently investigated with a suitably large sample.

(iv) A possible additional URC physical parameter (e.g. the surface stellar density) to take care of the (small) variance of the RCs profiles that seems to be unaccounted by the luminosity.

Finally, let us remind the reader that, in a flat cosmology with matter density parameter $\Omega_{\text{M}} = 0.27$ and Hubble constant $H_0 = 71 \text{ km s}^{-1} \text{ Mpc}^{-1}$, at the present time, the halo virial radius R_{vir} , that is, the size of the virialized cosmological perturbation of mass M_{vir} scales with the latter as

$$R_{\text{vir}} = 259 \left(\frac{M_{\text{vir}}}{10^{12} M_{\odot}} \right)^{1/3} \text{ kpc} \quad (4)$$

(see e.g. Eke et al. 1996).

2 THE UNIVERSAL HALO VELOCITY PROFILE

We assume that the DM MD is described by the Burkert profile

$$\rho(r) = \frac{\rho_0 r_0^3}{(r+r_0)(r^2+r_0^2)}, \quad (5a)$$

where r_0 is the core radius and ρ_0 the effective core density, in principle two independent parameters. Correspondingly, the total halo mass inside radius r is given by $M_{\text{H}}(r) = 4 M_0 [\ln(1 + \frac{r}{r_0}) - \tan^{-1}(\frac{r}{r_0}) + \frac{1}{2} \ln(1 + \frac{r^2}{r_0^2})]$ with $M_0 = 1.6 \rho_0 r_0^3$, so that

$$V_{\text{URCH}}^2(r) = 6.4 G \frac{\rho_0 r_0^3}{r} \left\{ \ln \left(1 + \frac{r}{r_0} \right) - \tan^{-1} \left(\frac{r}{r_0} \right) + \frac{1}{2} \ln \left[1 + \left(\frac{r}{r_0} \right)^2 \right] \right\}. \quad (5b)$$

Inside R_l this profile is indistinguishable from the halo term (2b) in the URC₀ (Salucci & Burkert 2000; Gentile et al. 2004). At larger radii, the mass diverges only logarithmically with radius and converges to the NFW velocity profile, provided that $r_0 \ll R_{\text{vir}}$.

We fit the set of individual and co-added RCs of PSS with $V_{\text{URC}}(R; M_{\text{D}}, \rho_0, r_0)$ and derive the model parameters $M_{\text{D}}, \rho_0, r_0$ (see Salucci & Burkert 2000):

$$\log \frac{\rho_0}{\text{g cm}^{-3}} = -23.515 - 0.964 \left(\frac{M_{\text{D}}}{10^{11} M_{\odot}} \right)^{0.31} \quad (6a)$$

and

$$\rho_0 = 5 \times 10^{-24} r_0^{-2/3} e^{-(r_0/27)^2} \text{ g cm}^{-3}. \quad (6b)$$

Equations (1), (2a), (5b), (6a) and (6b) define the URC out to R_l , $V_{\text{URC}}(R, M_{\text{D}}, r_0)$, from the ‘baryonic perspective’. Let us notice that (as a result of modelling the RC mass) r_0 , differently from M_{D} and ρ_0 , has quite large fitting uncertainties, namely, $\delta r_0/r_0 = 0.3-0.5$. Following our empirical approach, we do not extrapolate the URCH determined inside R_l out to $R_{\text{vir}} \gg R_l$, because this will be uncertain as well as of unknown validity. This quantity will be derived in the next section.

3 THE URC OUT TO THE VIRIAL RADIUS

We overcome the two main limitations of the URC₀, its problematic extrapolation between R_l and R_{vir} and the uncertainty in the estimate of the core radius, by determining the latter by means of a new *outer* observational quantity, the halo virial velocity $V_{\text{vir}} \equiv [GM_{\text{vir}}/R_{\text{vir}}(M_{\text{vir}})]^{1/2}$, related to the virial mass through equation (4). In detail, we obtain V_{vir} from the disc mass, suitably measured from inner kinematics through its relationship to the virial mass found by Shankar et al. (2006):

$$M_{\text{D}} = 2.3 \times 10^{10} M_{\odot} \frac{[M_{\text{vir}}/(3 \times 10^{11} M_{\odot})]^{3.1}}{1 + [M_{\text{vir}}/(3 \times 10^{11} M_{\odot})]^{2.2}}. \quad (7)$$

This relationship is a consequence of the existence of (i) the universal stellar mass function, (Bell et al. 2003; Baldry et al. 2004) and of (ii) the cosmological halo mass function as indicated by N -body Λ CDM simulations.³ Let us notice that this relationship is obtained without assuming any halo density profile, so that it can be combined with the mass modelling of the inner kinematics.

Let us first derive $R_{\text{D}}(M_{\text{vir}})$, the disc scalelength as a function of the halo mass, by inserting equation (7) in the relationship

$$\log \frac{R_{\text{D}}}{\text{kpc}} = 0.633 + 0.379 \log \frac{M_{\text{D}}}{10^{11} M_{\odot}} + 0.069 \left(\log \frac{M_{\text{D}}}{10^{11} M_{\odot}} \right)^2 \quad (8)$$

obtained in PSS. We note that no result of this work is affected by the observational uncertainties on the relationship equation (8).

It is worth to compute the radial extrapolation needed to reach R_{vir} from $R_l = 6R_{\text{D}}$, a quantity that can also be associated with the baryonic collapse factor $F = R_{\text{vir}}/R_{\text{D}}$; we find $F \approx 90 - 15 \log \frac{M_{\text{vir}}}{10^{11} M_{\odot}}$, that is, about 25 times the disc size $\sim 3 R_{\text{D}}$.

Equation (7) in combination with equation (4) allows us to add, to the PSS set of kinematical data leading to the URC₀, a new observational quantity: $V_{\text{vir}}(M_{\text{D}}) = GM_{\text{vir}}/R_{\text{vir}}$, relative to the virial radius. Then, we determine the core radius not from the inner kinematics, but as the value of r_0 for which the velocity model described by equations (1), (2a), (5b) and (6a), matches (at R_{vir}) the virial velocity V_{vir} given by equations (7) and (4). Let us write this as

$$\frac{GM_{\text{vir}}}{R_{\text{vir}}(M_{\text{vir}})} = V_{\text{URCH}}^2 [R_{\text{vir}}(M_{\text{vir}}); \rho_0(M_{\text{vir}}, r_0)], \quad (9a)$$

where $\rho(M_{\text{vir}})$ as a short form for $\rho(M_{\text{D}}(M_{\text{vir}}))$ with equation (7) inserted in equation (6a). From the PSS inner kinematics we get the values of ρ_0 and M_{D} according to equation (6a), so that equation (9a) becomes an implicit relation between r_0 and M_{vir} (c_1, c_2 are known numerical constants):

$$M_{\text{vir}} = c_1 \frac{\rho_0(M_{\text{vir}}) r_0^3}{c_2 M_{\text{vir}}^{1/3}} \left\{ \ln \left(1 + \frac{c_2 M_{\text{vir}}^{1/3}}{r_0} \right) - \tan^{-1} \left(\frac{c_2 M_{\text{vir}}^{1/3}}{r_0} \right) + \frac{1}{2} \ln \left[1 + \left(\frac{c_2 M_{\text{vir}}^{1/3}}{r_0} \right)^2 \right] \right\}. \quad (9b)$$

The above can be numerically solved for any M_{vir} , and the solution can be approximated by

$$\log (r_0/\text{kpc}) \simeq 0.66 + 0.58 \log \frac{(M_{\text{vir}})}{10^{11} M_{\odot}}. \quad (10)$$

³ There is no inconsistency in adopting the Λ CDM halo mass function or cored halo mass models, in that the latter can be formed astrophysically from the cosmological cuspy distributions. Since both functions account the same cosmological objects, the Jacobian of their transformation defines a relation between the disc and virial mass in spirals (see Shankar et al. 2006).

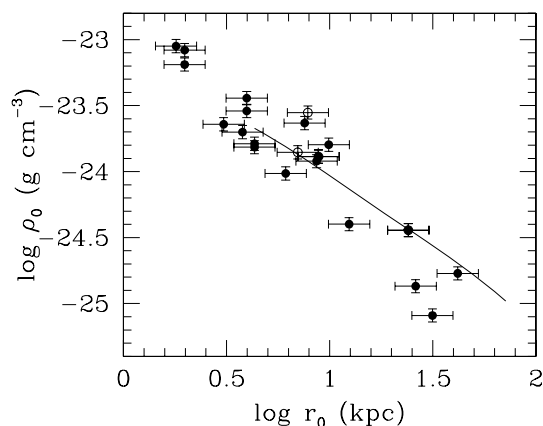


Figure 1. The core radius versus virial mass relations for the SE sample and the present work (solid line).

Let us stress that the present derivation of r_0 is very solid with respect to observational uncertainties: errors up to a factor 2 in M_{vir} in equation (7) trigger errors in r_0 lower than 40 per cent, and errors in the outer halo velocity slope ($0.1 \leq R/R_{\text{vir}} \leq 1$) lower than 0.1. This is certainly smaller than the scatter of values with which this quantity is found by N -body simulations and by smoothed particle hydrodynamics/semi-analytical studies of galaxy formation including the baryonic components.

It is worth investigating a number of recently published superextended (SE) RCs (Salucci et al. 2003; Gentile et al. 2004; Donato et al. 2004). They reach a radius larger than 5 per cent (and up to 15 per cent) of the virial radius, that is, a radius at least twice as extended as those of the synthetic curves in PSS. The mass modelling of these SE RCs (made in the original papers) shows an r_0 versus M_{vir} relationship that is in good agreement with equation (10) (see Fig. 1). Relation (10) and the above individual values differ by 20–40 per cent from those determined from the inner kinematics alone and given by means of equation (6b). Since in this paper (also because $R_l \sim r_0$), equations (6a) and (6b) are considered a prediction of the inner mass modelling rather than an actual measurement, such good agreement indicates the soundness of the PSS mass modelling.

Let us notice that only for a range of values of the crucial quantity $V(R_l) - V_{\text{vir}}$, with the first term obtained by the inner kinematics and the second one via equations (4) and (7), there is a solution for equation (9b), therefore, the existence of equation (10) and the agreement of the values of the Burkert core radii, measured independently at $0.05R_{\text{vir}}$, $0.1R_{\text{vir}}$ and R_{vir} are important tests passed by this profile.

Then, by means of equations (1), (2a), (5b), (6a) and (10), we construct the full URC, extended out to the virial radius and with the virial mass as the galaxy indicator. It is useful to show the relationships we use (see Fig. 2). The mass model includes a Burkert DM halo of central density ρ_0 , of core radius of size r_0 and a Freeman disc of mass M_{D} . The URC fits nicely the available velocity data out to R_l and it is valid out to the virial radius, where it exactly matches V_{vir} . Moreover, since M_{vir} is the quantity that in theoretical studies identifies a galaxy, we overcome the main limitation of URC₀.

We consider all of the three coordinate systems $r, r/R_{\text{D}}, r/R_{\text{vir}}$ equivalent to represent the main structural properties of the MD in spirals, but each of them showing some particular aspects. More specifically, it is then possible and useful to build several ‘URCs’, that is, $V_{\text{URC}}(r/R_{\text{coo}}; P)$, where P is a galaxy identifier ($M_{\text{D}}, M_{\text{vir}}, L$) and R_{coo} a radial coordinate ($r, r/R_{\text{D}}, r/R_{\text{vir}}$). Although not all these

URCs are independent in a statistical sense, they all are relevant in that they all well reproduce the individual RCs and each of them highlights particular properties of the MD.

In Fig. 3 we show $V_{\text{URC}}(r; M_{\text{vir}})$, the URC in physical units with the objects identified by the halo virial mass; each line refers to a given halo mass in the range $10^{11} M_{\odot} \lesssim M_{\text{vir}} \lesssim 10^{13} M_{\odot}$; the halo mass determines both the amplitude and the shape of the curve. Note the contribution of the baryonic component, negligible for small masses but increasingly important in the larger structures, mirrors the behaviour of the $M_{\text{vir}}-M_{\text{D}}$ relation. The general existence of an inner peak is evident but, especially at low masses, it is due to both dark and stellar components. Remarkably, the maximum value of the circular velocity occurs at about 15 ± 3 kpc, independent of the galaxy mass: this seems to be a main kinematic imprint of the DM – luminous mass interaction occurring in spirals. Furthermore, Fig. 3 shows that the ‘cosmic conspiracy’ paradigm has no observational support: there is no fine tuning between the dark and the stellar structural parameters to produce the same particular RC profile in all objects (e.g. a flat one). Conversely, a number of relationships between the various structural parameters produce a variety of RC profiles. Moreover, the peak velocity of the stellar component $V_{\text{disc}}^{\text{peak}} = V_{\text{D}}(2.2 R_{\text{D}}) = GM_{\text{D}}/R_{\text{D}}k$, with $k = \text{constant}$, is not a constant fraction of the virial velocity as is found in ellipticals (i.e. $\sigma \propto V_{\text{vir}}$), but it ranges between the values 1 and 2 depending on the halo mass.

Moreover, as in the NFW (and Burkert) RC profiles, the URC profiles are found (moderately) decreasing over most of the halo radial extent. The paradigm of flat RCs is obviously incorrect even/especially intended as an asymptotic behaviour at large radii. In fact, we find that both $V(0.05 R_{\text{vir}})$, the velocity at the farthest radius with available kinematical in PSS and $V(3R_{\text{D}})$, a main reference velocity of the luminous regions of spirals, are significantly (10–30 per cent) higher than the (observational) value of V_{vir} . This rules out a $V = \text{constant}$ extrapolation of the inner RCs out to regions non-mapped by the kinematics and DM dominated regions. We note that this result is independent of the adopted halo density profile and is far from being granted on theoretical grounds.

In Fig. 4 we frame the URC from a full DM perspective by plotting $V_{\text{URC}}(R/R_{\text{vir}}; M_{\text{vir}})$. We set the virial mass M_{vir} as the galaxy identifier and R/R_{vir} as the radial ‘dark’ coordinate, thus normalizing the amplitudes by $V_{\text{vir}} \propto M_{\text{vir}}^{1/3}$. This ensemble of curves, a main goal of the present work, is parallel to those emerging in N -body simulations and aims to represent the actual velocity profiles of spi-

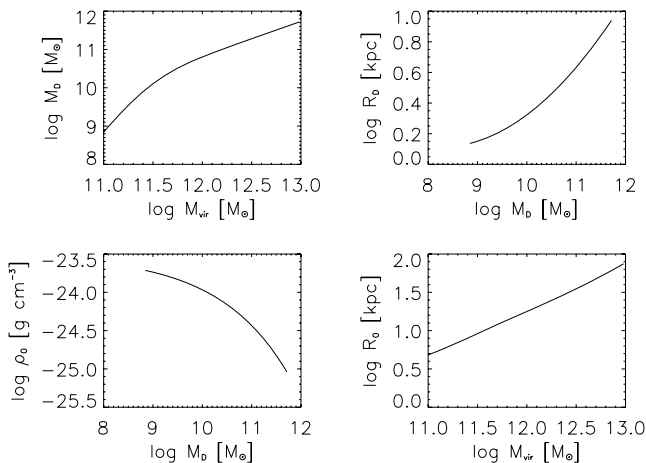


Figure 2. The various relationships used in this paper.

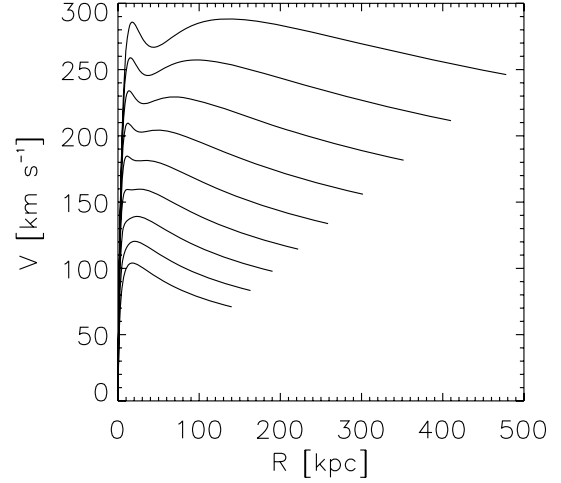


Figure 3. The URC in physical units. Each curve corresponds to $M_{\text{vir}} = 10^{11} 10^{n/5} M_{\odot}$, with $n = 1-9$ from the lowest to the highest curve.

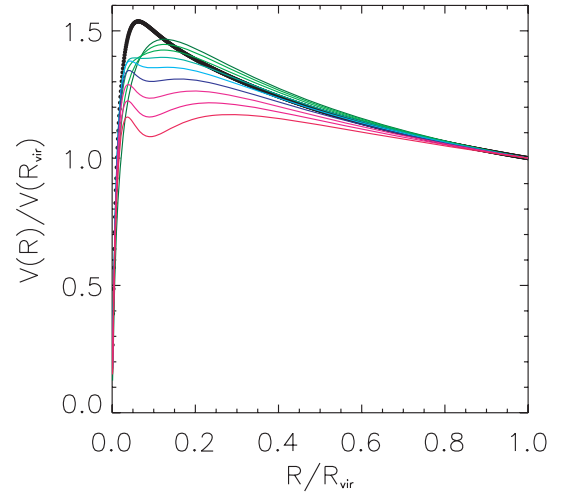


Figure 4. The URC, normalized at its virial value $V_{\text{URC}}(R_{\text{vir}})$, as a function of normalized dark radius $x \equiv R/R_{\text{vir}}$. Each curve, from the highest to the lowest, corresponds to M_{vir} defined as in Fig. 3. The bold line is the NFW velocity profile (see text).

erals. In these variables the DM haloes are self-similar; the whole system is self-similar in the outer regions, while in the innermost 30 per cent of the halo size the baryons have influenced the dynamics and broken the self-similarity. From these coordinates it easily emerges that the maximum of the RC occurs at very different radii, namely, at $\simeq 2 R_{\text{D}}$ for the most massive objects and at $\sim 10 R_{\text{D}}$ for the least massive ones. Then, no reference circular velocities, which should be considered as the actual physical counterparts of the empirical velocities of the Tully–Fisher relationship, exist in actual galaxy RCs.

In Fig. 5 we zoom into the URC to look for the inner (luminous) regions of spirals from a baryonic perspective: the URC is so expressed as a function of the ‘baryonic’ radial coordinate r/R_{D} . This figure corresponds to Fig. 4 of PSS, with the important difference that here the virial mass, rather than the galaxy luminosity, is the galaxy identifier. Plainly, an inverse correlation between the average steepness of the RC slope and the halo mass holds, similar to the slope–luminosity relationship found by Persic & Salucci (1988). In this coordinate the stellar matter is closely self-similar, and the

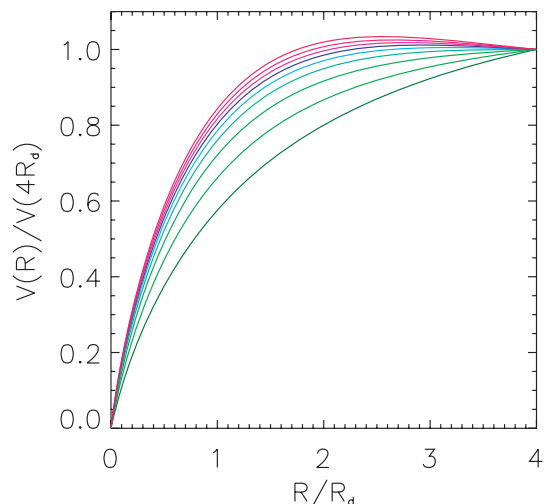


Figure 5. The inner URC, normalized at its value at $4R_D$, as a function of normalized stellar radius R/R_D for galaxies with M_{vir} as in Fig. 3.

different shapes of the RCs are mainly due to the $M_{\text{vir}}-M_D$ relation. In the space defined by normalized circular velocity–dark radius–halo mass, spirals do not occupy random positions, but a well-defined plane of very small thickness. We clearly see that, by filling only less than 10^{-3} per cent of the available volume, the available kinematics of spiral galaxies defines the URC. Let us notice that, in principle, theories of the formation of spirals do not trivially imply the existence of such a surface that underlies the occurrence of a strong dark-luminous coupling.

We now show the URC DM density distribution. In Fig. 6 we show it as a function of x and M_{vir} . For $x < 10^{-1}$ the well known core–cusp discrepancy emerges, that is, the DM density of actual haloes around spirals is about one order of magnitude smaller and radially much more constant than the NFW predictions. At $x > 0.4$, for a concentration parameter $c = 13 (M_{\text{vir}}/10^{12} M_{\odot})^{-0.13}$, the observed halo densities are consistent with the NFW predictions for haloes of the same virial mass. Note that this is a direct test: for haloes with density profiles at $x > 0.5$ very different from the Burkert or the NFW profiles, equation (9b) does not have solution.

More specifically, let us constrain the analytical form of the outer DM distribution. For $2 \leq r/r_0 \leq 18$, the following approximation for the Burkert and NFW profile holds ($y \equiv r/r_0$, $\epsilon = 0$)

$$V_{\text{URCH}}(y) = V_{\text{URCH}}(3.24) \frac{2.06 y^{0.86}}{1.59 + y^{1.19+\epsilon}}. \quad (11)$$

Let us suppose that the actual *outer* DM velocity profile is different from the Burkert/NFW given by equation (11), that is, $\epsilon \neq 0$. Then in Fig. 7 we show that, even assuming large uncertainties in V_{vir} , in order to match both $V(R_i)$ and V_{vir} , we must have $\epsilon < 0.1$. This is a first direct support for the Burkert and the NFW density law to be able to represent the outer regions ($0.3 \leq r/R_{\text{vir}} \leq 1$) of DM galaxy haloes.

Notice that weak-lensing shear fields, at several hundreds kpc from the galaxy centres, are found *compatible* with the predictions of the NFW density profile, but cannot exclude non-NFW profiles (Kleinheinrich et al. 2006, and references therein).

4 DISCUSSION AND CONCLUSIONS

In this paper, we have built the URC of spiral galaxies by means of kinematical and photometric data. We physically extended the

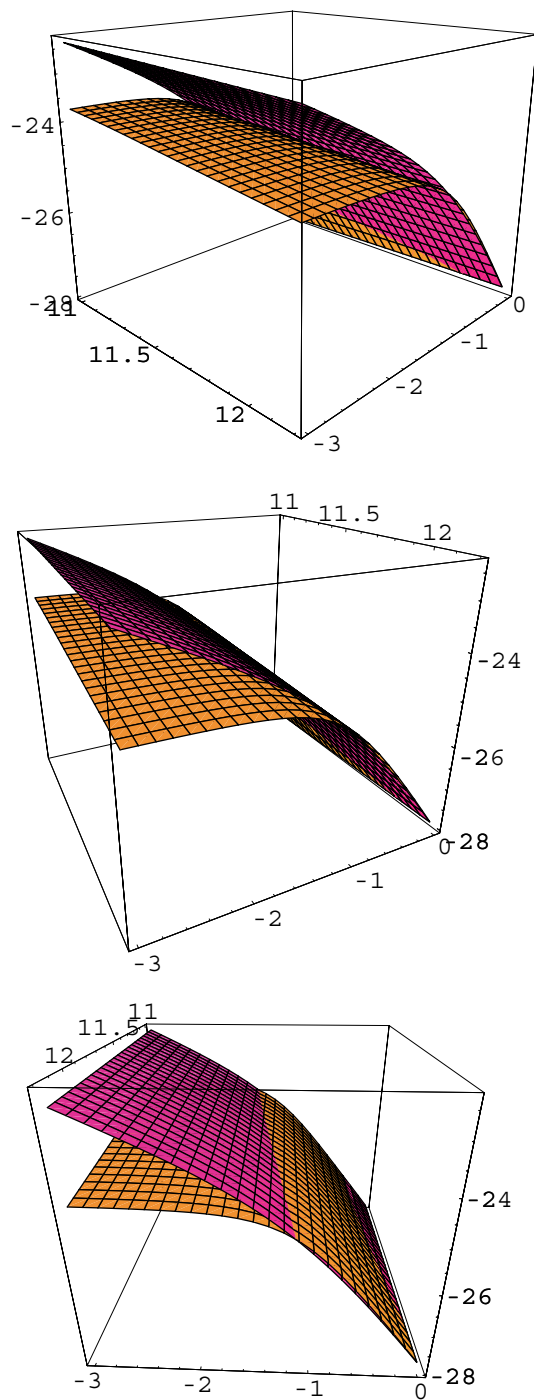


Figure 6. The URC halo density versus the NFW halo density of objects of the same mass, as a function of normalized radius and virial mass. The axes labels are x , $\log M_{\text{vir}}/M_{\odot}$ and $\log(\rho/(\text{g cm}^{-3}))$

URC, established for the inner region of galaxies in PSS out to R_{vir} and have been able to employ the virial mass M_{vir} as the parameter that characterizes spiral galaxies, and the virial radius R_{vir} as a unit of measure for the radial coordinate. This URC is meant to be the *observational* counterpart of the NFW RC, emerging from cosmological simulations performed in the CDM scenario. The URC yields the gravitational potential at any radius and it allows us to link

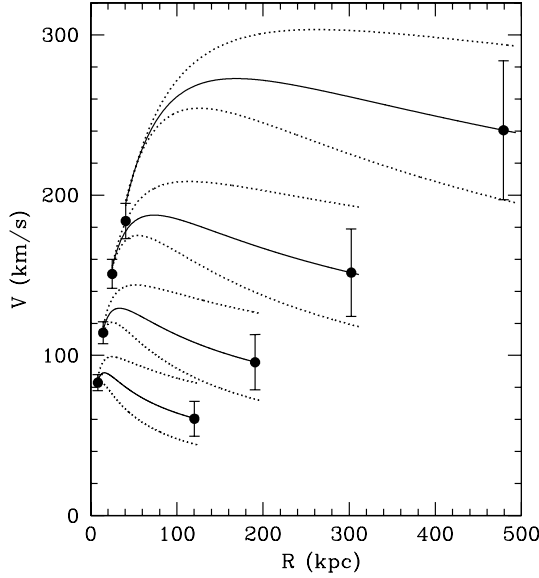


Figure 7. Halo velocities at R_l and R_{vir} (filled circles) versus the URC-halo velocity, given by equations (11) (solid line) and versus velocity profiles with average logarithmic slope steeper or shallower by an amount $\epsilon = 0.1$ (dashed line).

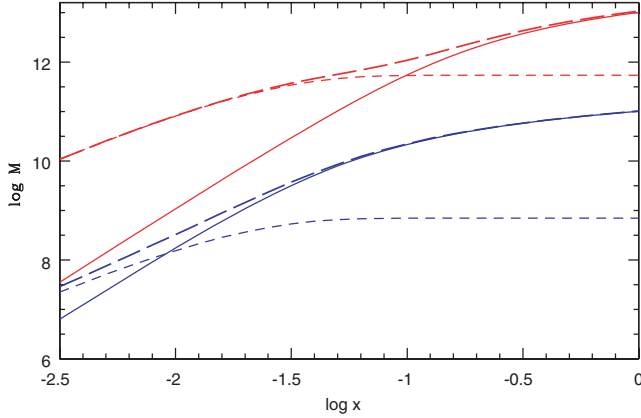


Figure 8. The dark halo (solid line), the disc (short dashed line) and the total (long dashed) URC mass profile for reference masses of 10^{11} and $10^{13} M_{\odot}$. The distribution for the intermediate halo masses can be derived from Section 2.

the local properties in the inner luminous regions with the global properties of the DM haloes.

DM haloes have one (and likely just one) characteristic length-scale, $r_0 \propto M_{\text{vir}}^{0.6}$, which it is not *naturally* present in current scenarios of galaxy formation. Thus, they do not show any sign of an inner cuspy region of size $r_s \propto M_{\text{vir}}^{0.4}$. The halo velocity contribution V_{URCH} rises with radius like a solid body at $r \sim 0$, decelerates to reach a maximum at $3.24 r_0$ from where it starts to slowly decrease out to R_{vir} with a slope that it is consistent with that of the NFW haloes. The main significance of the URC concerns the full MD. First, it is possible to immediately exclude the following scenarios (and combinations of them): (i) individual behaviour, every object has its own MD; (ii) unique behaviour, every object has almost the same MD. Instead, the MD in spirals shows a remarkable *mass-dependent* systematics: both the dark and the stellar matter are distributed according to *profiles* that are functions of the total mass M_{vir} (see Fig. 8). Finally, the DM halo becomes the dominant mass component in galaxies at

different radii, according to the galaxy mass: from $\sim 10^{-2} R_{\text{vir}}$ for the lowest masses, to $\sim 10^{-1} R_{\text{vir}}$ for the highest ones.

We write the equilibrium velocity of the haloes around spirals as the following approximation of the relations in the previous section:

$$V_{\text{URCH}} = A(M_{\text{vir}})x^{-1/2} \left\{ \ln[1 + \gamma(M_{\text{vir}})x] - \tan^{-1}[\gamma(M_{\text{vir}})x] + \frac{1}{2} \ln[1 + \gamma(M_{\text{vir}})x^2] \right\}^{0.5}$$

with $A(M_{\text{vir}}) = 0.406 + 1.08 \log[M_{\text{vir}}/(10^{11} M_{\odot})] - 0.688 \{\log[M_{\text{vir}}/(10^{11} M_{\odot})]\}^2 + 0.766 \{\log[M_{\text{vir}}/(10^{11} M_{\odot})]\}^3$ and $\gamma(M_{\text{vir}}) = 26.78 [M_{\text{vir}}/(10^{11} M_{\odot})]^{-0.246}$. This is the observational counterparts of N -body outcomes.

A MATHEMATICA code for the figures in this paper is available at <http://www.novicosmo.org/salucci.asp>.

ACKNOWLEDGMENTS

We thank L. Danese for helpful discussions, and the referee for useful comments.

REFERENCES

- Baldry I. K., Glazebrook K., Brinkmann J., Ivezić Z., Lupton R. H., Nichol R. C., Szalay A. S., 2004, *ApJ*, 600, 681
- Bell E. F., McIntosh D. H., Katz N., Weinberg M. D., 2003, *ApJS*, 149, 289
- Borriello A., Salucci P., 2001, *MNRAS*, 323, 285
- Bosma A., 1981, *AJ*, 86, 1791
- Broeils A. H., 1992a, *A&A*, 256, 19
- Broeils A. H., 1992b, PhD thesis, Groningen Univ.
- Bullock J. S., Kolatt T. S., Sigad Y., Somerville R. S., Kravtsov A. V., Klypin A. A., Primack J. R., Dekel A., 2001, *MNRAS*, 321, 559
- Catinella B., Giovanelli R., Haynes M. P., 2006, *ApJ*, 640, 751
- Courteau S., 1998, *AJ*, 114, 2402
- Donato F., Gentile G., Salucci P., 2004, *MNRAS*, 353, 17
- Dutton A. A., van den Bosch F. C., Dekel A., Courteau S., 2007, *ApJ*, 645, 27
- Eke V. R., Cole S., Frenk C. S., 1996, *MNRAS*, 282, 263
- Freeman K. C., 1970, *ApJ*, 160, 811
- Gentile G., Salucci P., Klein U., Vergani D., Kalberla P., 2004, *MNRAS*, 351, 903
- Gentile G., Burkert A., Salucci P., Klein U., Walter F., 2005, *ApJ*, 634, L145
- Gentile G., Salucci P., Klein U., Granato G. L., 2007, *MNRAS*, 375, 199
- Kleinheinrich M. et al., 2006, *A&A*, 455, 441
- Mo H. J., Mao S., White S. D. M., 1998, *MNRAS*, 295, 319
- Navarro J. F., Frenk C. S., White S. D. M., 1996, *ApJ*, 462, 563
- Noordermeer E., 2007, *MNRAS*, in press (astro-ph/0701731)
- Persic M., Salucci P., 1988, *MNRAS*, 234, 131
- Persic M., Salucci P., 1990, *MNRAS*, 245, 577
- Persic M., Salucci P., 1991, *ApJ*, 368, 60
- Persic M., Salucci P., 1995, *ApJS*, 99, 501
- Persic M., Salucci P., Stel F., 1996, *MNRAS*, 281, 27 (PSS)
- Rhee M.-H., 1996, PhD thesis, Groningen Univ.
- Roscoe D. F., 1999, *A&A*, 343, 788
- Rubin V. C., Ford W. K. Jr, Thonnard N., 1980, *ApJ*, 238, 471
- Rubin V. C., Ford W. K. Jr, Thonnard N., Burstein D., 1982, *ApJ*, 261, 439
- Rubin V. C., Burstein D., Ford W. K., Jr, Thonnard N., 1985, *ApJ*, 289, 81
- Salucci P., Burkert A., 2000, *ApJ*, 537, L9
- Salucci P., Persic M., 1997, in Persic M., Salucci P., eds, *ASP Conf. Ser. Vol. 117, Dark and Visible Matter in Galaxies*. Astron. Soc. Pac., San Francisco, p. 1
- Salucci P., Walter F., Borriello A., 2003, *A&A*, 409, 53
- Shankar F., Lapi A., Salucci P., De Zotti G., Danese L., 2006, *ApJ*, 643, 14

- Simon J. D., Bolatto A. D., Leroy A., Blitz L., Gates E. L., 2005, *ApJ*, 621, 757
- Swaters R. A., 1999, PhD thesis, Groningen University
- Swaters R. A., Madore B. F., van den Bosch F. C., Balcells M., 2003, *ApJ*, 583, 732
- Tonini C., Lapi A., Salucci P., 2006a, *ApJ*, 849, 591
- Tonini C., Lapi A., Shankar F., Salucci P., 2006b, *ApJ*, 638, L13
- van den Bosch F. C., Swaters R. A., 2001, *MNRAS*, 325, 1017
- Verheijen M., 1997, PhD thesis, Groningen Univ.
- Weldrake D. T. F., de Blok W. J. G., Walter F., 2003, *MNRAS*, 340, 12
- Willick J. A., 1999, *ApJ*, 516, 47
- Yegorova I., Salucci P., 2006, *MNRAS*, submitted (astro-ph/0612434)

APPENDIX

In this appendix we discuss the observational evidence for the URC claim, the nature and the implications of which it is worth to clarify. The paradigm states that, when binned by luminosity, the RCs form a set of smooth, low-scatter synthetic curves, whose profiles and amplitudes are strong functions of the luminosity bin.⁴ Furthermore, the URC paradigm implies: (i) rotation velocity slopes *versus* rotation velocity amplitudes relationships (see figs 2 and 3 of PSS) and (ii) a set of relations (radial Tully–Fisher relationship) holding at different radii x , defined as

$$\log V(x) = a_x M + b_x,$$

where $x \equiv R/R_D$ and a_x and b_x are the fitting parameters, and M is the galaxy magnitude (Persic & Salucci 1991).

Evidence for the URC claim and/or its above implications comes from: (i) detailed analyses of independent samples: Catinella et al. (2006), (2200 RCs, see their fig. 12), Swaters (1999), (60 extended RCs, see chapter 4); (ii) independent analyses of the PSS sample:

Rhee (1996), Roscoe (1999); (iii) the finding of a very tight RTF in PSS and other three different samples Willick (1999, see below), Yegorova et al. (2006).

The claim has been also tested by comparing the RCs of two samples of spirals (Courteau 1998, 131 objects; Verheijen 1997, 30 objects) with the circular velocities predicted by the URC_0 , once that the values of galaxy luminosity and disc length-scale are inserted in it. The face-value result of the test: 2/3 of the RCs are in pretty good agreement with the universal curve, while 1/3 show some disagreement, indicates that the URC is a useful tool to investigate the systematics of the MD in spirals, but also it questions about its universality. However, while some of this disagreement may reflect an inefficiency of the URC_0 to reproduce the RCs, the actual performance of the URC is better than it is claimed. In fact, spurious data versus predictions disagreements are created in performing this test and precisely when they insert in URC_0 the values of L_B and R_D , affected by (occasionally large) observational errors. By taking into account this effect the URC_0 success rate reaches 80 per cent and more.

Willick (1999) found, by studying a large sample of RCs, a radial variation of the scatter of the inverse RTF defined above and he interpreted it as an evidence against the URC. Let us show that this argument is incorrect and that *au contraire* the properties of the RTF support the URC paradigm. The increase/decrease of the scatter found is very small (Willick 1998): the scatter ranges from 0.065 dex (at $2R_D$) to 0.080 dex (at $0.5R_D$ and at $3R_D$) and it implies, if totally intrinsic, a prediction error in $\log V(x)$ of $(0.08^2 - 0.065^2)^{0.5} = 0.04$ dex. Moreover, some of the scatter increase/decrease is due to the larger random observational errors present in the outermost measurements; in fact, a refined analysis of the issue (Yegorova et al. 2006) finds a smaller predicting error for three large sample of spirals. Therefore, from the RTF we have that, in the region considered, the luminosity *statistically* predicts the circular velocity at any radius and in any galaxy within an error of 5–10 per cent, a quantity much smaller than the variations of the latter *in each galaxy and among galaxies*.

This paper has been typeset from a $\text{\TeX}/\text{\LaTeX}$ file prepared by the author.

⁴ The *analytical form* of the URC is built by assuming reasonable disc–halo velocity profiles, with three free parameters [$V(R_{\text{opt}})$, a , β] that are obtained by χ^2 -fitting the synthetic curves.